Data Science in Finance and Economics

https://www.aimspress.com/journal/dsfe

DSFE, 5(3): 419–439.
DOI: 10.3934/DSFE.2025017
Received: 03 May 2025
Revised: 07 August 2025
Accepted: 19 September 2025
Published: 25 September 2025

*Research article*

# Regime-Specific interdependencies in cryptocurrency markets: A high-frequency GMM-VAR approach

**Prashant Joshi***

Department of Accounting and Finance, School of Business, Saint Martin's University, WA 98503, USA

* **Correspondence**: Email: pjoshi@stmartin.edu.

**Abstract**: In this study, we examined the regime-dependent dynamics and interrelationships among major cryptocurrencies, Bitcoin (BTC), Ethereum (ETH), and Monero (XMR), using high-frequency one-minute data from January 2020 to April 2025. To capture the presence of latent structural shifts without assuming Markovian transitions, we employed a Gaussian Mixture Model (GMM), which flexibly clustered distributions into two, empirically distinct regimes. Regime-specific Vector Autoregressive (VAR) models were then estimated to analyze interdependencies, spillovers, and shock transmission mechanisms across these digital assets. In the calm regime, the return dynamics were primarily self-driven, with limited cross-asset responses. Conversely, the volatile regime exhibited stronger and more persistent interlinkages, with BTC consistently acting as the principal transmitter of shocks to ETH and XMR, while ETH acts as a secondary transmitter, whereas XMR remains largely a risk recipient, absorbing external shocks with limited feedback into the system. These findings were corroborated through impulse response functions and forecast error variance decompositions, which consistently revealed asymmetric interdependence structures across the regimes. The Granger causality indicated more stable and statistically significant causal relationships in the calm regime than in the volatile regime. Furthermore, the Bai-Perron structural break tests confirmed the absence of significant deterministic breaks in the return series, reinforcing the validity of the GMM-based regime identification. These findings have practical implications for investors, regulators, and risk managers when modeling contagion and developing risk management strategies in cryptocurrency markets, especially during periods of heightened volatility.

**Key Words**: Cryptocurrency markets; High frequency data; Gaussian Mixture Model (GMM); Regime identification; Vector Autoregression (VAR)

**JEL classification**: C32, C38, C51, C58, G15

## 1. Introduction

Cryptocurrencies represent a significant innovation in the financial sector, providing a decentralized form of currency that operates independently of governmental control (Alzahrani and Daim, 2019). The market has grown dramatically, with increasing adoption levels and interest from both individual and institutional investors (Mungo et al., 2024**)**. Bitcoin, Ethereum, and Tether collectively represent 79.26% of the market capitalization (Statista, 2025). Blockchain technology guarantees data integrity, security, and decentralized storage across distributed networks (Meunier, 2018). Bitcoin (BTC), Ethereum (ETH), and Litecoin (LTC) are among the most significant among the many cryptocurrencies (Council, 2021). Trading in cryptocurrencies involves substantial risk owing to highly volatile price movements and unpredictable market dynamics (Kochliaridis et al., 2024). Extreme price volatility acts as a major motivation and a considerable barrier to market participation (Hadan et al., 2024).

Owing to the highly volatile nature of cryptocurrencies, researchers have employed statistical models to understand cryptocurrency market dynamics. Volatility modeling primarily relies on GARCH models (Katsiampa et al., 2019; Guesmi et al., 2019; Bouri et al., 2020), whereas interdependencies among cryptocurrencies have been examined using vector autoregressive (VAR) models (Ji et al., 2018; Yi et al., 2018), and the Granger Causality test (Mgadmi et al., 2024) has been applied to understand market interconnections. However, reliance on daily close prices within short durations may affect the ability of studies to identify long-term trends and limit their generalizability of the results. Although these models are beneficial, they may not adequately reflect the complex dynamics of cryptocurrency markets over a long duration. By extending the models to include long-term perspectives and intraday data, we can gain valuable insights into the market dynamics.

Building on traditional volatility models, quantile regression (Koenker and Bassett, 1978) and its extensions, such as the Conditional Autoregressive Value at Risk (CAViaR) model (Engle and Manganelli, 2004), have been extensively applied to traditional financial assets (White et al., 2015). However, their application in the cryptocurrency markets remains limited. Several researchers (Taylor, 2019; Merlo et al., 2021) have built on the CAViaR framework to improve VaR and expected shortfall (ES) forecasting. Advancements have introduced expectile regression as a more flexible approach to capture nonlinear tail dependencies in market data (Foroni et al. 2024). However, these studies often fail to consider the impact of regime shifts on asset behavior, which we address in this study.

Given the limitations of traditional approaches in capturing regime shifts, regime-switching models have gained prominence in financial research (Hamilton, 1989,1994). These models characterize the dynamics of financial returns that are influenced by regimes, making them well-suited for highly volatile assets such as cryptocurrencies.

Figá-Talamanca and Patacca (2019) investigated the influence of market attention on Bitcoin returns and volatility using daily data. Pennoni et al. (2022) identified six distinct regimes, consisting of three positive and three negative states. Nonetheless, both investigations are based on daily data collected over a relatively brief period, which may not adequately capture the long-term dynamics inherent in these markets. Oelschläger and Adam (2023) introduced hierarchical hidden Markov models (HMMs) to differentiate short-term price fluctuations and long-term trends in financial time series data. However, the focus on the two hierarchical structures and the assumption of conditional independence across financial time series may not reflect the complex interdependencies.

Agakishiev et al. (2025) introduced a regime-switching reinforcement learning model and applied it on Bitcoin metadata, hourly CRIX cryptocurrency index and Bitcoin price data. They found the potential benefits of the model for investment management. However, owing to the nonstationary nature of cryptocurrency markets, achieving accurate predictions may remain challenging. Similarly, Turatti et al. (2025) explored Duration-dependent Markov switching (DDMS) models for capturing volatility clustering effects. However, the selection of appropriate duration parameters is complex and subjective, leading to computational challenges that can limit the model's scope.

Hidden Markov Models (HMMs) play an essential role in the examination of longitudinal data and in describing dynamic heterogeneity (Zou et al., 2024). They can model time-series processes that switch between several latent states (Aarts and Hasibeck, 2024).

However, HMMs have certain limitations. One drawback is the assumption that the next state is influenced solely by the current state, disregarding any effects from previous states. This characteristic of 'memorylessness' may not accurately capture the intricate dependencies and long-term patterns often found in financial time series data (Esmael et al., 2012; Johnson & Willsky, 2013, Yuksel et al., 2015; Li, 2023, Dimri et al., 2024).

While regime-switching models based on Markov chains have gained traction in the cryptocurrency literature (Ma et al., 2020; Figà-Talamanca et al., 2021; Kim et al., 2022; Mgadmi et al., 2023), their reliance on Markovian transition assumptions may not always reflect the empirical dynamics of high-frequency financial data. To address this, we adopt a Gaussian Mixture Model (GMM) approach for regime identification. Unlike HMMs, GMMs enable the direct clustering of return distributions without assuming time-dependent transitions between regimes. This flexibility makes GMMs particularly effective for high-frequency financial data, where structural breaks and volatility shifts may not follow sequential patterns. Notably, Kalliovirta et al. (2016) developed the GMM-VAR framework, which unites GMM-based regime identification with VAR-based interdependency modeling using interest rate and exchange rate data. This hybrid approach facilitates smooth transitions and allows for state-specific estimation of VAR parameters, offering improved empirical fit and interpretability.

In the context of regime identification, GMMs offer a tractable alternative to the more complex Markov-switching models. Gaussian mixture models can be used to approximate asset-return distributions (Zhang & Cheng, 2003). Wong and Chan (2005) demonstrated the superiority of mixture Gaussian processes in capturing long-term dynamics of the S&P 500 and Toronto Stock Exchange indices.

The GMM can approximate skewed return distributions and model different market regimes effectively (Tan and Chu, 2012; Wang et al., 2025). Eirola and Lendasse (2013) employed GMMs for time-series interpolation and forecasting, highlighting their strength in handling complex temporal dependencies.

The application of GMMs to high-frequency data has gained popularity in recent years. GMMs adapt more quickly to significant market changes and can be significantly superior to other widespread VaR methods in predicting market risk (Morkūnaitė et al., 2024). Scrucca (2024) examined the applications of Gaussian mixtures in modeling the empirical distribution of financial log-returns and in deriving traditional risk measures. This study highlights the benefits of GMMs in effectively capturing the complex and dynamic nature of financial data.

The GMM-VAR framework offers key methodological improvements over traditional Markov-switching VAR (MS-VAR) and Bayesian Hidden Markov Models (HMMs) that rely on time-dependent transition probabilities and strict Markovian assumptions, enforcing rigidity on regime dynamics. Such rigidity may limit their ability to capture abrupt, non-sequential, and overlapping regime shifts that are characteristic of high-frequency cryptocurrency markets. In contrast, our use of GMM enables unsupervised distribution-based regime identification without requiring fixed temporal dependencies. This data-driven flexibility enables improved detection of nonlinearities, multimodal structures, and structural breaks in asset returns that may go undetected in MS-VAR or HMM-based approaches.

By integrating GMM with VAR, we isolate distinct volatility regimes and characterize inter-asset return dynamics conditional on those regimes, a feature not naturally embedded in pure clustering models. This two-step approach enables flexible regime discovery and dynamic interaction modeling, offering a novel hybrid structure that is particularly suited to high-frequency cryptocurrency data.

Compared to alternative unsupervised methods, GMM offers distinct advantages. While k-means clustering assigns data points to clusters based on distance without considering uncertainty in transitions (Bishop, 2006; Reynolds, 2009; Tengelin & Sopasakis, 2020), GMM enables soft clustering with interpretable probabilistic membership. The interpretability of GMM-based regime identification makes it attractive for risk management applications. While Dirichlet Process Mixture Models (DPMMs) provide nonparametric flexibility (Gershman & Blei, 2011), they face computational and interpretability challenges in settings with overlapping clusters (Lee and kim, 2023) and the need for clear regime labeling, as required in VAR estimation.

Moreover, our framework addresses the key limitations of applying unsupervised learning to financial time series by bridging statistical learning with economic interpretability. The GMM enables closed-form likelihood estimation, which supports formal model selection and provides a clear delineation of calm and volatile periods for downstream VAR modeling.

Although most researchers focus on Bitcoin, this narrow focus restricts a better understanding of cryptocurrencies and their applications in the real world. Furthermore, researchers have relied heavily on daily data, limiting its ability to capture intraday market fluctuations and short-term shifts in the regimes. Additionally, the reliance of most researchers on daily data limits their ability to capture intraday market fluctuations and short-term regime shifts.

Here, we address these gaps by leveraging a high-frequency dataset with 1-minute intervals to cover short-term regime shifts in BTC, ETH, and XMR prices. These cryptocurrencies are selected for their distinctive roles within the digital asset ecosystem. Bitcoin, the most widely held and traded cryptocurrency, is a proxy for the overall market sentiment and systematic risk (Corbet et al., 2018). Ethereum, which represents the largest smart contract platform, captures exposure to decentralized finance, innovation-driven volatility, and technology-related narratives (Ante, 2021). In contrast, Monero is a privacy-oriented cryptocurrency, often characterized by unique regulatory sensitivities and a relatively lower correlation with mainstream digital assets (Wang et al., 2023). Although XMR's trading volume is lower than that of BTC and ETH, its inclusion introduces valuable asset heterogeneity, enabling us to examine whether regime-dependent interdependencies manifest differently across tokens with diverse market microstructures. This broader scope facilitates the exploration of asymmetric dependencies under varying volatility regimes and enhances the robustness of our findings. Unlike researchers who rely on either Hidden Markov Models (HMM) or Markov-Switching Autoregression (MS-VAR), we employ a GMM in combination with regime-specific VAR analysis. This hybrid GMM-VAR framework offers a more flexible and realistic representation of cryptocurrency price dynamics across volatility regimes, enhancing the robustness of our results and supporting more effective risk modeling and trading strategy development, thereby improving predictive performance and trading strategy development.

The remainder of this paper is organized as follows. In Section 2, we outline the materials and methods used in this study. In Section 3, we present the empirical results. In Section 4, we provide a detailed discussion of the findings and some future research directions.

## 2. Materials and methods

In this section, we outline the data sources, preprocessing steps, and the methodological framework employed in the analysis. In Section 2.1, we describe the dataset. In Section 2.2, we present the econometric methodology, including regime identification using the GMM and regime-specific VAR modeling. Figure 1 illustrates the overall GMM-VAR workflow employed in this study.


**Figure 1**. GMM-VAR Framework.

### *2.1. Data description*

We employ high-frequency, one-minute interval closing price data for BTC, ETH, and XMR, spanning January 1, 2020, to April 25, 2025. The data are obtained from the EOD historical data (https://eodhd.com) and converted into logarithmic returns.

### *2.2. Methodology*

#### 2.2.1. GMM for regime identification

We use a GMM framework to uncover latent regimes in high-frequency cryptocurrency return data. The GMM is an unsupervised learning technique that enables the identification of latent regimes in the absence of pre-labeled training data. This approach is particularly well-suited for financial time series data, where regime labels are not directly observable. The GMM assumes that observed returns are generated from a mixture of multiple multivariate normal distributions, each of which represents a different market regime. Unlike the Hidden Markov Model (HMM), the GMM used here does not model the transition probabilities or time dependence between regimes. Instead, regime classification is based on the posterior probabilities of component membership.

Formally, the likelihood of an observation $x_t$ is modeled as

$$p(x_t) = \sum_{k=1}^{K} \pi_k \ \mathcal{N}( x_t \mid \mu_k, \Sigma_k ) \tag{1}$$

where $\pi_k$ is the mixing proportion of regime k, such that

$$\sum_{k=1}^{K} \pi_k = 1$$

Here, $\mu_k$ and $\Sigma_k$ are the mean vector and covariance matrix of the Kth Gaussian component, respectively. K is the total number of regimes in this model. It was selected by comparing models with different components using the Akaike Information Criterion (AIC) and the Bayesian Information Criterion (BIC). $\mathcal{N}( x_t \mid \mu_k, \Sigma_k )$ denotes the multivariate normal density.

The model parameters $\{\pi_k, \mu_k, \Sigma_k\}_{k=1}^{K}$ *are* estimated using the Expectation-Maximization (EM) algorithm (Dempster et al., 1977). Each observation $x_t$ is assigned to regime k, which maximizes the posterior probability as follows:

$$\gamma_k(x_t) = \frac{\pi_k \mathcal{N}( x_t | \mu_k, \Sigma_k )}{\sum_{j=1}^{K} \pi_j \mathcal{N}\left( x_t | \mu_j, \Sigma_j \right)} \tag{2}$$

2.2.2. Regime-Specific VAR modeling

Following the identification of regimes using GMM, we estimate a VAR framework (Sims, 1980) to capture regime-dependent interactions. The VAR framework enables the intercept, autoregressive coefficients, and variance-covariance matrices to vary across regimes. The VAR(p) process can be described as follows:

$$\Phi(L) Y_t = \varepsilon_t \tag{3}$$

where $Y_t = (Y_{1t}, Y_{2t}, \dots, Y_{kt})$ represents a stationary ( n × 1) vector of k time series containing *n* observations, and where $\varepsilon_t = (\varepsilon_{1t}, \varepsilon_{2t}, \dots, \varepsilon_{kt})$ is an (n × 1) is a vector of random shocks, which are independently and identically distributed, following a normal distribution with a mean of zero and a covariance of Σ. The matrix Φ(L) is a full rank (k × k) matrix that includes autoregressive parameters and is characterized by finite polynomial elements in the lag operator L. $Y_t$ can be interpreted as a response to a stochastic input $\varepsilon_t$, while the matrix Φ(L) delineates the adjustment patterns to these shocks. The stationarity properties of the individual time series are assessed using an augmented Dickey-Fuller (Dickey et al., 1979, 1981). The lag structure within the VAR system is determined using the AIC and BIC. The effects of shocks on various cryptocurrencies are examined using a variance decomposition method. Specifically, the variance of the t-year forecasting errors of variable *i, as* explained by innovations in variable *j, is* as follows:

$$\frac{\sum_{e=0}^{t-1} c_{ij}(r)^2}{\sum_{j=1}^{k} \sum_{r=0}^{t-1} c_{ij}(r)^2} \tag{4}$$

where $c_{ij}(r)$ is the (i, j) components of the (k × k) matrix $C(r)$ and represents the dynamic response of each endogenous variable $Y_t$ to a shock, $u_j(t-s)$, after s periods. $c_{ij}(r)$ is an orthogonalized moving average representation of $Y_t$, which is defined as:

$$Y_t = \sum_{s=0}^{\infty} C(r)u(t-r) \tag{5}$$

The responses to shocks in a variable is represented by coefficients of $C(r)$ following orthogonalization, while orthogonalized residuals are contained within $u(t-r)$.

## 3. Results

In this section, we present the results of our empirical analyses. In Section 3.1, we detail the outcomes of the descriptive statistics of the cryptocurrency return series. In Section 3.2, we test for stationarity using the Augmented Dickey-Fuller (ADF) test. In Section 3.3, we report the results of the Bai-Perron structural break test. We identify the regimes using GMM in Section 3.4. In Section 3.5, we focus on the estimation of regime-specific VAR models, including an analysis of the impulse response functions (IRFs) and forecast error variance decompositions (FEVDs). Finally, in Section 3.6, we present the results of the Granger causality test.

### *3.1. Descriptive statistics*

We begin our empirical analysis by presenting the descriptive statistics for BTC, ETH, and XMR returns. We utilize intraday one-minute interval closing price data spanning January 1, 2020, to April 25, 2025. The initial exploration highlights the key distributional characteristics of the data, including measures of central tendency, dispersion, and tail behavior.

**Table 1**. Descriptive statistics of cryptocurrency returns.

| Asset | Mean | Standard Deviation | Skewness | Kurtosis |
|---|---|---|---|---|
| Bitcoin (BTC) | 0.00000107 | 0.0011573 | 0.16533 | 296.19 |
| Ethereum (ETH) | 0.000000990 | 0.0013787 | −0.67498 | 275.62 |
| Monero (XMR) | 0.00000427 | 0.0012924 | 0.63937 | 234.49 |

Table 1 reports the descriptive statistics, indicating that all series exhibit near-zero mean returns and high kurtosis, suggesting the presence of extreme return events. Skewness varies across assets, with Ethereum displaying negative skewness, while Bitcoin and Monero exhibiting positive skewness.

### *3.2. Stationarity tests (ADF)*

Stationarity is a crucial requirement for numerous time-series models because it ensures that the series demonstrates consistent behavior over time. In this study, we employ the ADF test to assess whether the returns of BTC, ETH, and XMR exhibit stationarity. The ADF test is represented as

$$\Delta y_t = \alpha + \beta t + \gamma y_{t-1} + \sum_{i=1}^{p} \delta_i \Delta y_{t-i} + \varepsilon_t \quad (6)$$

where $y_t$ is the series being tested, α is a constant, $\beta_{t-1}$ represents a deterministic trend, γ is the coefficient on the lagged level of the series (testing for stationarity), $\delta_i$ are the coefficients for lagged differences, and $\varepsilon_t$is the white noise error term.

The ADF test evaluates the null hypothesis that a unit root is present in the time series, indicating nonstationarity. By including lagged differences of the variable, the test accounts for potential autocorrelation in the error term. The test is applied separately to the returns of BTC, ETH, and XMR. The results of the ADF test are presented in Table 2.

**Table 2**. ADF Test results.

| Asset | ADF Statistics | |
|---|---|---|
| | Intercept* | Trend* |
| BTC | −1945.21 | −1945.21 |
| ETH | −1877.45 | −1877.85 |
| XMR | −1874.10 | −1874.12 |

**All values are significant at 1% level*

The null hypothesis is rejected at a 1% significance level for all return series across both regimes, indicating that the series are trend stationary. Accordingly, the series are linearly detrended before further analysis.

### *3.3. Structural break test*

Before proceeding with regime identification and the estimation of the VAR model, it is essential to evaluate the temporal stability of the return series. Financial time series, such as cryptocurrencies, are susceptible to abrupt shifts owing to regulatory interventions, technological changes, or market-wide events. The presence of structural breaks can lead to biased parameter estimates and misleading inferences. We employ the Bai-Perron test (Bai and Perron, 1998, 2003) to identify unknown structural changes in the return series, ensuring that subsequent analysis is conducted for a stable data-generating process.

The general regression model with m breaks is specified as follows:

$$y_t = X_t' \beta_j + \varepsilon_t, \quad \text{for } T_{j-1} < t \le T_j, \quad j = 1, \dots, m+1 \quad (7)$$

where $y_t$ is the dependent variable, $X_t$ is the vector of regressors, $\beta_j$ is the vector of coefficients for regime j, $T_j$ is the breakpoint, and $\varepsilon_t$ is the error term. The test statistic is constructed by comparing the residual sum of squares (RSS) of the segmented model to that of a constant-coefficient model, with the optimal number of breaks selected using an information criterion, such as the Bayesian Information Criterion.

The Bai-Perron test was applied to the BTC, ETH, and XMR return series. Based on the Bayesian Information Criterion (BIC), the optimal number of breakpoints was zero for all three series in this study. The results indicate that the return-generating processes for all three cryptocurrencies remained statistically stable over the selected sample period. Therefore, these series can be considered structurally stable for subsequent analyses.

### 3.4. *Regime identification using GMM*

We employ a GMM to capture the latent volatility regimes in BTC, ETH, and XMR returns. Model selection using the Bayesian Information Criterion (BIC) initially indicates that a five-regime specification is optimal. However, the empirical estimation of the five-regime model reveals that two of the regimes contain no observations (Appendix A, Table A1), while another regime exhibits near-zero variance across all assets (Appendix A, Table A2), suggesting a lack of substantive economic meaning. Similar instability persists when fitting the four-and three-regime models. Based on these empirical considerations, we select a two-regime model that distinctly captures “calm” periods of low volatility and “volatile” periods characterized by heightened market fluctuations.

Table 3 presents the estimated mean returns and covariance matrices for both regimes. The calm regime is characterized by lower mean returns and reduced covariances, whereas the volatile regime demonstrates higher mean returns and elevated covariances across assets.

**Table 3.** Mean returns and covariance matrices across regimes.

| Regime | BTC Return | ETH Return | XMR Return |
|---|---|---|---|
| Calm Regime | 0.0925 | 0.0911 | 0.4065 |
| Volatile Regime | 0.2119 | 0.1140 | 0.2951 |
| Calm Regime Covariance | 0.1315 | 0.0869 | 0.0381 |
| | 0.0869 | 0.1868 | 0.0481 |
| | 0.0381 | 0.0481 | 0.1648 |
| Volatile Regime Covariance | 0.3663 | 0.1686 | 0.1226 |
| | 0.1686 | 0.4920 | 0.1419 |
| | 0.1226 | 0.1419 | 0.3287 |

Note: Mean returns are expressed in $10^{-5}$ and $10^{-3}$ scales; covariances are expressed in $10^{-5}$ and $10^{-4}$ scales for the calm and the volatility regimes, respectively.

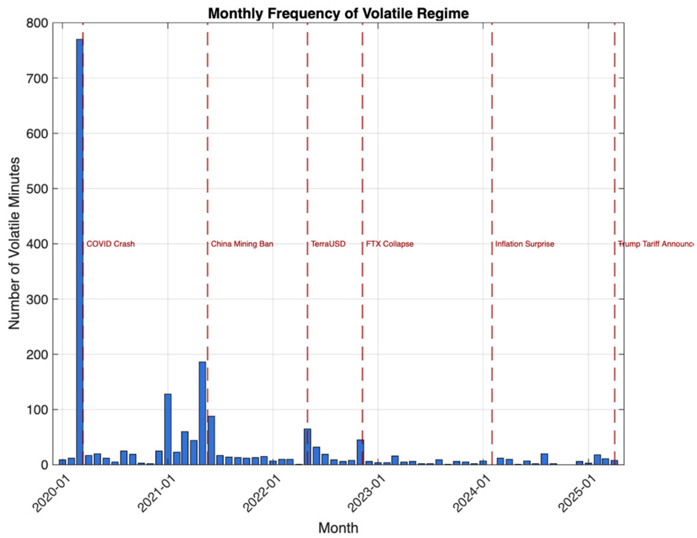


**Figure 2**. Monthly frequency of volatile regime.

We conduct a detailed analysis of the volatility regime by plotting the monthly frequency of minutes classified as the volatile regime (Figure 2). The figure reveals that major market disruptions, such as the COVID-19 crash, China mining ban, TerraUSD collapse, FTX collapse, inflation surprise, and news related to tariffs, are associated with pronounced surges in the occurrence of volatile episodes.

### *3.5. VAR model estimation and diagnostics*

To examine the interdependencies among cryptocurrency returns across regimes, we estimate VAR models separately for the calm and volatile regimes, as identified by the GMM. VAR models enable us to capture the dynamic interactions among cryptocurrencies through IRFs and FEVD. In addition, Granger causality tests are conducted to assess the direction and significance of causal relationships among the return series.

Although the VAR model facilitates the dynamic modeling of regime-specific interdependencies, it is inherently linear, which may not fully capture the nonlinear dependencies and jump-driven dynamics present in high-frequency financial data. Nonetheless, this simplifying assumption enables a tractable estimation and clearer interpretation of cross-asset relationships.

To enhance robustness in our empirical framework, we apply multiple pre-processing and diagnostic checks, including VAR stability tests, optimal lag length selection, unit root testing (ADF), structural break analysis, and residual diagnostics. We further strengthen the inference by implementing wild bootstrap methods (Gonçalves & Kilian, 2004) to generate confidence bands for regime-specific IRFs and FEVDs. This approach accounts for heteroskedasticity and non-Gaussian features in high-frequency returns, offering more reliable inferences under structural volatility. These procedures ensure the adequacy and robustness of the estimated regime-specific VAR models.

#### 3.5.1. Lag length selection and VAR estimation

Prior to estimating the VAR models, the optimal lag length is determined using the Akaike Information Criterion (AIC), which provides a balance between the model fit and complexity. The AIC suggests a lag length of five for both the calm and volatile regimes. Consequently, we estimate the VAR(5) models separately using the linearly detrended return series for BTC, ETH, and XMR. The stationarity of the models is verified by examining the eigenvalues of their companion matrices. In both regimes, all eigenvalues are strictly within the unit circle, confirming the stationarity of the VAR systems.

#### 3.5.2. Residual diagnostics

To assess the adequacy of the estimated VAR(5) models, we conduct a residual diagnostic test. The Ljung-Box-Q test (Ljung & Box, 1978) is applied to determine whether the residuals exhibit autocorrelation. Table 4 presents the p-values across all assets and regimes.

**Table 4**. Ljung-Box-Q test results.

| Regime | Asset | p-value |
|---|---|---|
| Calm | BTC | 0.21 |
| | ETH | 0.94 |
| | XMR | 0.57 |
| Volatile | BTC | 0.85 |
| | ETH | 0.44 |
| | XMR | 0.54 |

The results fail to reject the null hypothesis of no autocorrelation at the 5% level for BTC, ETH, and XMR in either regime. This suggests that the residuals are serially uncorrelated, indicating well-specified models.

### 3.5.3 ARCH effects

To evaluate the presence of conditional heteroskedasticity in the residuals across each regime, we perform ARCH LM (Engle, 1982) tests for BTC, ETH, and XMR. The findings presented in Table 4 indicate the presence of volatility clustering in both the calm and volatile regimes.

**Table 5**. ARCH LM test results for residuals.

| Regime | Asset | p-value |
|---|---|---|
| Calm | BTC | 0.00 |
| | ETH | 0.00 |
| | XMR | 0.00 |
| Volatile | BTC | 0.00 |
| | ETH | 0.00 |
| | XMR | 0.00 |

Note: The null hypothesis of no ARCH effect is rejected at the 1% level for all the series.

We implement a residual-based wild bootstrap with Rademacher weights to account for conditional heteroskedasticity in high-frequency data. For each replication, the bootstrap residuals are generated as follows:

$$\widehat{\varepsilon_t} = (\widehat{\varepsilon_{1t}}, \widehat{\varepsilon_{2t}}, \dots, \widehat{\varepsilon_{kt}})^{T} \tag{8}$$

$$\varepsilon_t^* = \omega_t \cdot \widehat{\varepsilon_t} \tag{9}$$

$$y_t^* = \sum_{i=1}^{p} \widehat{A}_i\, y_{t-i}^* + \varepsilon_t^*, \quad t = p + 1, \dots, T. \tag{10}$$

where ωt ~ Rademacher($\pm 1$) and $\widehat{A}$ are estimated VAR coefficients. This process is used to generate empirical distributions of regime-specific IRFs and FEVDs.

### 3.5.4. Impulse response function analysis

To investigate the dynamic interactions among cryptocurrency returns, we compute IRFs based on the estimated VAR(5) models for each regime using wild bootstrapping inference to account for heteroskedasticity. IRFs reveal how shocks to one cryptocurrency affect itself and others over time under different regimes, enabling a more granular understanding of temporal shock propagation.

Figure 3 displays the orthogonalized IRFs across both regimes. The left and right panels correspond to the calm and volatile regimes, respectively. Each subplot illustrates the response of a given variable to a one-standard-deviation shock in another variable over a 20-minute horizon. The volatile regime exhibits stronger and more persistent interdependencies than the calm regime.

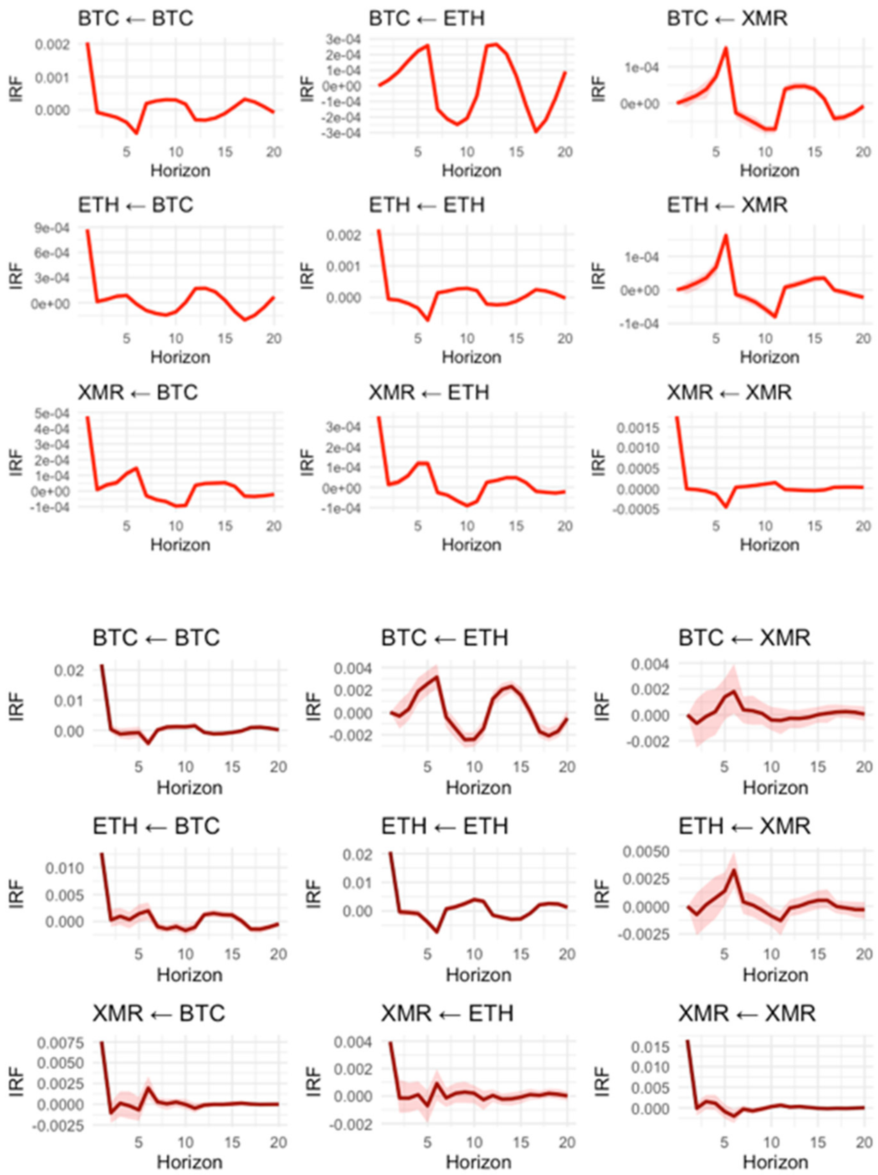


**Figure 3**. Impulse response functions across regimes at 95% CI (note: The left panels correspond to the calm regime, and the right panels correspond to the volatile regime).

In the calm regime, shocks to the BTC return generates modest and short-lived responses in ETH and XMR, indicating limited cross-asset spillovers under low-volatility conditions. Similarly, shocks to ETH lead to mild responses in BTC and XMR, with the effects dissipating quickly. XMR responses to external shocks are minimal, reinforcing its relatively isolated behavior in tranquil market states. All responses returned to the baseline quickly, which is consistent with the weak dynamic interactions in the calm regime.

In contrast, the volatile regime exhibits more pronounced and persistent responses. A one-standard-deviation shock to BTC leads to immediate and substantial effects for both ETH and XMR, highlighting BTC’s role as the primary transmitter of volatility during market stress. ETH’s sensitivity to BTC shocks intensifies in this regime, with significant responses sustained across horizons. Similarly, XMR becomes notably more responsive to shocks originating from BTC and ETH, particularly in the early post-shock period. These results underscore BTC's central role of BTC as a volatility transmitter during stress episodes. Although ETH and XMR shocks also influence other assets, and the magnitude and persistence of these effects underline a shift toward greater systematic interconnectedness and contagion during high-volatility periods.

The confidence bounds of the IRFs differ markedly across regimes. In the calm regime, responses are tightly bounded, indicating low uncertainty and rapid reversion to equilibrium. By contrast, the volatile regime exhibits wider confidence intervals, especially for ETH and XMR responses to BTC shocks, underscoring the heightened uncertainty and persistence of interdependencies during stress periods.

The IRFs provide compelling evidence of asymmetric interdependencies that become more pronounced under stress. BTC emerges as the dominant influencer of volatility across regimes. ETH acts as a secondary transmitter, whereas XMR remains largely a risk recipient, absorbing external shocks with limited feedback into the system. These regime-dependent IRF patterns emphasize the importance of accounting for time-varying interdependencies when modeling and managing risk in crypto markets.

### 3.5.5. Forecast error variance decomposition

To further explore the regime-specific dynamics of shock transmission, we perform a FEVD based on the estimated VAR(5) models for calm and volatile regimes. FEVD enables us to quantify the proportion of forecast error variance in each cryptocurrency that can be attributed to innovations in itself and other cryptocurrencies.

As illustrated in Figure 4, the calm regime is characterized by a strong own-variance dominance. Specifically, shocks to BTC account for over 95% of its forecast error variance, with negligible contributions from ETH and XMR, which explain approximately 85% and 88% of their return variances, respectively. The influence of other cryptocurrencies is modest. BTC explains approximately 22% of the variance in ETH and about 10% in XMR, whereas ETH and XMR contribute minimally to each other’s return variances and to BTC. The dominance of own shocks suggests weak spillovers and low systemic integration under stable market conditions.

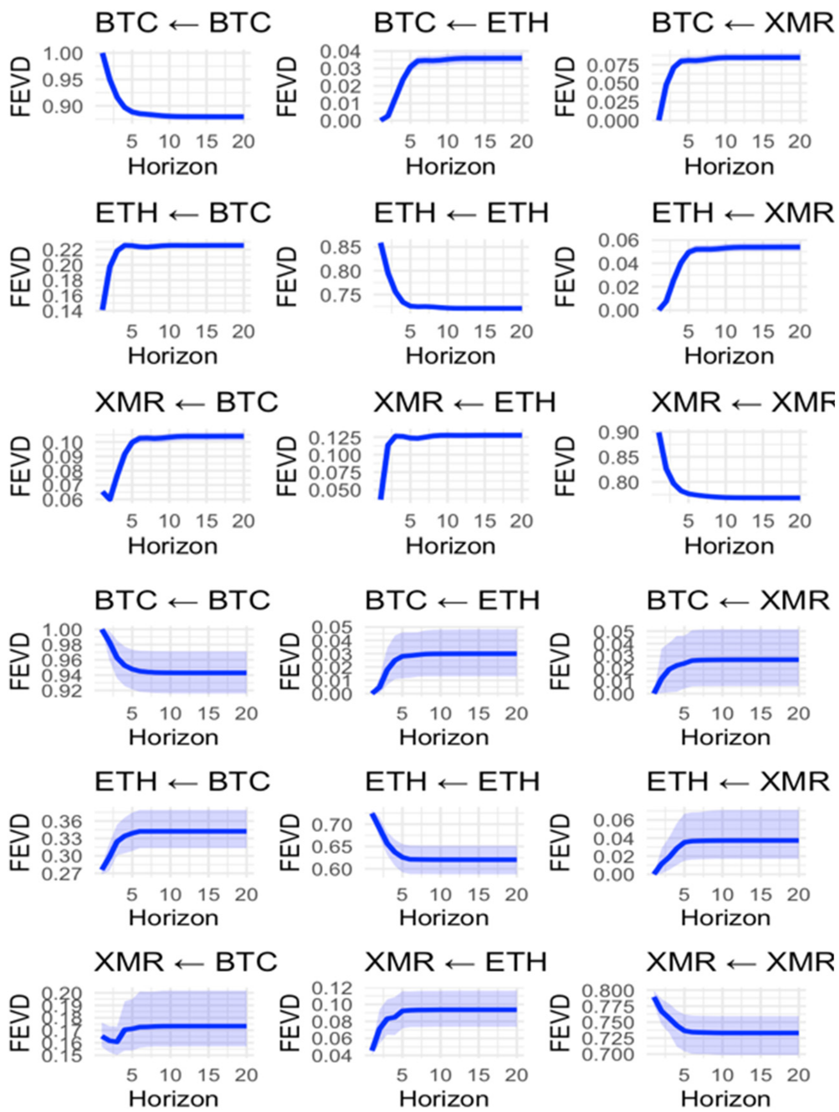


**Figure 4**. Forecast Error Variance Decomposition (FEVD) across regimes at 95% CI (note: The left panels correspond to the calm regime, and the right panels correspond to the volatile regime).

In contrast, the volatile regime demonstrated markedly higher levels of interconnectedness. BTC continues to emerge as a dominant source of volatility transmission. BTC explains over 92% of its own forecast error variance, but its contribution to the forecast variances of ETH and XMR increases significantly. BTC accounts for nearly 36% of ETH's variance and approximately 20% of XMR's, highlighting its central role as a systemic risk transmitter during stress. ETH's influence also grows modestly, contributing approximately 5% to BTC's variance and about 12% to XMR's. However, XMR continues to play a passive role, primarily absorbing volatility from BTC and ETH while adding little to their return variances.

In addition to the point estimates, the width of the confidence bands in the FEVD plots exhibits significant variation across regimes. In the calm regime, the bands are narrow, indicating stable and predictable variance contributions. Conversely, in the volatile regime, the confidence intervals expand considerably, reflecting heightened uncertainty in the transmission of shocks. This underscores the necessity of regime-specific modeling and highlights the advantage of employing wild bootstrap inference to capture the heteroskedasticity and fat-tailed behavior characteristic of high-frequency cryptocurrency markets.

These findings confirm the regime-dependent nature of the interdependencies among cryptocurrencies and underscore the dominant role of BTC, particularly during market stress, in shaping the volatility structure of the crypto ecosystem.

### *3.6. Granger causality*

To assess the predictive relationship among the cryptocurrency returns, we employ Granger causality tests within the VAR(5) framework originally proposed by Granger (1969). The Granger causality test determines whether the past values of one time series provide statistically significant information about the future values of another.

Granger causality is tested using the following regression equation:

$$Y_t = \alpha + \sum_{i=1}^{p} \beta_i Y_{t-i} + \sum_{i=1}^{p} \gamma_i X_{t-i} + \varepsilon_t \tag{11}$$

The above specification represents a typical Granger causality test, where $Y_t$ is regressed on its own lagged values and the lagged values of another variable $X_t$. If the $\gamma_t$ on the lagged $X_t$ terms are jointly statistically significant, we reject the null hypothesis and conclude that X Granger-causes Y.

To a*ddress* the ARCH-type heteroscedasticity, inference is conducted using robust methods consistent with our bootstrap-based approach applied throughout the VAR analysis.

The test results are presented in Table 6.

**Table 6**. Granger causality test results.

| Null Hypothesis | Regime | Chi-square (df = 5) | p-value |
|---|---|---|---|
| Lagged ETH does not Granger-cause BTC | Calm | 48446.00 | 0 |
| Lagged XMR does not Granger-cause BTC | Calm | 4713.40 | 0 |
| Lagged BTC does not Granger-cause ETH | Calm | 32680.00 | 0 |
| Lagged XMR does not Granger-cause ETH | Calm | 4210.60 | 0 |
| Lagged BTC does not Granger-cause XMR | Calm | 12392.00 | 0 |
| Lagged ETH does not Granger-cause XMR | Calm | 15743.00 | 0 |
| Lagged ETH does not Granger-cause BTC | Volatile | 25.412 | 0 |
| Lagged XMR does not Granger-cause BTC | Volatile | 35.15 | 0 |
| Lagged BTC does not Granger-cause ETH | Volatile | 46.56 | 0 |
| Lagged XMR does not Granger-cause ETH | Volatile | 33.81 | 0 |
| Lagged BTC does not Granger-cause XMR | Volatile | 54.02 | 0 |
| Lagged ETH does not Granger-cause XMR | Volatile | 99.38 | 0 |

In both regimes, we reject all null hypotheses of no Granger causality at the 1% significance level. This indicates a significant bidirectional causal relationship among all three cryptocurrencies in the calm and volatile regimes. The magnitude of the test statistics is notably higher during the calm regime, indicating stronger and more predictive relationships under calm market conditions. Although the relationships persist in the volatile regime, the reduced test statistics suggest that market stress may dampen the linear predictability among cryptocurrencies, possibly due to elevated noise or nonlinear dynamics. These findings underscore the importance of regime-sensitive modeling in analyzing interdependencies in crypto markets. These findings support and complement the impulse response and FEVD analyses, reinforcing the view that return spillovers are pervasive in cryptocurrency markets, regardless of the regime.

## 4. Discussion

In this study, we investigate the regime-dependent dynamics and interdependencies among major cryptocurrencies, BTC, ETH, and XMR, using high-frequency (1-minute interval) data from January 2020 to April 2025. By applying a GMM to the return series, we identify two distinct volatility regimes: Calm and volatile. Regime-specific VAR models are then employed to estimate interdependencies, enabling the analysis of IRFs, FEVD, and Granger causality tests.

Our findings reveal significant asymmetries in the market dynamics across regimes. During the calm regime, return dynamics are largely self-driven, with muted cross-asset interactions, consistent with weak spillover effects.

Conversely, the volatile regime exhibits stronger and more persistent cross-asset linkages. Shocks to BTC have substantial effects on ETH and XMR returns, as confirmed by the IRFs and FEVD results. The heightened interdependence observed in the volatile regime may be driven by a combination of external market-wide shocks and internal dynamics within cryptocurrency markets. The volatile regime identified in our analysis likely encapsulates market responses to several major shocks during the sample period, including the COVID-19 crash, China's cryptocurrency mining ban, the TerraUSD collapse, the FTX bankruptcy, inflation surprises, and tariff-related announcements. These events contribute to heightened uncertainty and reinforce the clustering of volatility and interdependencies across assets.

In addition to these external shocks, internal market dynamics likely play a role in amplifying interdependencies. Behavioral herding, liquidity clustering, and synchronized trading activity across exchanges can also intensify co-movements during stress periods. Traders often react simultaneously to macroeconomic announcements or cascading liquidations, increasing return interdependencies and reinforcing cross-asset spillovers. Moreover, algorithmic and high-frequency traders may rapidly adjust their portfolios during turbulence, further amplifying feedback loops. This confluence of behavioral dynamics and structural market microstructure effects can magnify regime-specific dependencies well beyond those observed in calmer market conditions.

Granger causality tests further validate the presence of statistically significant bidirectional relationships among the three assets during this regime. These results are consistent with the broader findings of previous regime-switching studies (Ma et al., 2020; Figà-Talamanca et al., 2021) while extending the literature by using intraday data and a GMM-based unsupervised learning approach that does not rely on the Markov assumption.

An important insight from the FEVD analysis is that ETH's role in shock transmission remains minor in both regimes, whereas BTC consistently emerges as the primary driver of this interdependence. This suggests a hierarchy in systemic influence among cryptocurrencies, highlighting Bitcoin's centrality in the crypto-financial ecosystem.

The incorporation of XMR into our analysis enhances our understanding of decentralized and privacy-oriented digital currencies within the broader crypto-financial context. During the calm regime, the XMR exhibits weak and short-lived responsiveness to shocks from BTC and ETH, indicating relatively low interdependence and reinforcing its more isolated role.

In contrast, under volatile conditions, XMR becomes more reactive to shocks from BTC and ETH while exerting limited influence in return. The findings underscore Monero's role as a risk recipient rather than a transmitter, especially during turbulent periods. While Monero may not serve as a conduit for systemic risk, it remains susceptible to systemic changes and external contagion within the broader crypto market. Consequently, its distinct behavior from BTC and ETH provides critical evidence of asymmetric and diverse market interdependencies among asset classes within the cryptocurrency domain.

The Bai-Perron test for structural breaks reveals no statistically significant breakpoints in the conditional mean of the return series, lending further support to the use of a regime-switching framework than adjusting for exogenous structural changes. This complements the unsupervised regime identification via GMM, affirming that the latent volatility regimes detected are inherent features of the data than artifacts of structural breaks. To address the challenges of inference in high-frequency cryptocurrency data, we employ wild bootstrap methods for both IRFs and FEVDs across calm and volatile regimes. This approach enhances the statistical reliability of our findings by accounting for variance instability and the behavior of heavy-tailed residuals. Specifically, it mitigates issues arising from non-Gaussian and heteroskedastic shocks, which are prevalent in ultra-high-frequency contexts. These methodological improvements substantiate the asymmetric transmission dynamics identified in the regime-based analysis.

Our approach demonstrates that regime-dependent modeling using GMM-VAR is effective in capturing the asymmetric behavior and volatility clustering that are typical of cryptocurrency markets. These results have practical implications for traders, portfolio managers, and regulators seeking to understand contagion risks and dynamic linkages during periods of market turbulence.

We recognize that ultra-high-frequency data often exhibit microstructure noise, asynchronous trading effects, and potential liquidity distortions within each market regime. Furthermore, XMR's relatively low trading volume may affect the precision of VAR coefficients, particularly in volatile regimes. Nonetheless, its inclusion enables us to investigate the behavior of less liquid and structurally distinct cryptocurrencies during stress. The presence of XMR adds valuable heterogeneity and tests whether privacy focused tokens display different interdependency patterns compared to major assets. Looking ahead, alternative approaches, such as machine learning-based regime-switching models, threshold VAR-GMM, nonlinear VAR, or GARCH-based GMM frameworks, offer promising avenues for modeling within-regime nonlinear dynamics and enhancing model robustness.

In the future, researchers could explore hybrid models that integrate machine learning algorithms for regime classification and forecasting or incorporate macro-financial variables to investigate cross-market contagions. Additionally, expanding the scope to include a broader set of altcoins or applying the GMM-VAR methodology to decentralized finance (DeFi) tokens could yield insights into emerging segments of the digital asset ecosystem.

This study contributes greatly to our understanding of cryptocurrency market dynamics by introducing a flexible, regime-based, novel GMM-VAR framework tailored to 1-minute high-frequency data. The model captures both the temporal and structural nuances of inter-asset relationships under various market conditions. These findings underscore the importance of adaptive analytical approaches in this rapidly evolving market and provide a foundation for more sophisticated risk management, trading strategies, and regulatory frameworks in the digital asset space.

**Use of AI tools declaration**

The authors declare they have not used Artificial Intelligence (AI) tools in the creation of this article.

**Conflict of interest**

The authors declare no conflict of interest.

**References**

Aarts E, Haslbeck JMB (2024) Modelling Psychological Time Series with Multilevel Hidden Markov Models: A Numerical Evaluation and Tutorial. *PsyArXiv.* https://doi.org/10.31234/osf.io/y2u5s

Agakishiev I, Härdle WK, Becker D, et al. (2025) Regime switching forecasting for cryptocurrencies. *Digit Financ* 7: 107–131. https://doi.org/10.1007/s42521-024-00123-2

Alzahrani S, Daim TU (2019) Analysis of the Cryptocurrency Adoption Decision: Literature Review. *2019 Portland International Conference on Management of Engineering and Technology (PICMET)*, 1–11. https://doi.org/10.23919/PICMET.2019.8893819

Ante L (2021) Smart contracts on the blockchain – A bibliometric analysis and review. *Telemat Inform* 57: 101519. https://doi.org/10.1016/j.tele.2020.101519

Bai J, Perron P (1998) Estimating and Testing Linear Models with Multiple Structural Changes. *Econometrica* 66: 47. https://doi.org/10.2307/2998540

Bai J, Perron P (2003) Computation and analysis of multiple structural change models. *J Appl Econometrics* 18: 1–22. https://doi.org/10.1002/jae.659

Bishop CM (2006) *Pattern Recognition and Machine Learning.* Springer.

Bouri E, Lucey B, Roubaud D (2020) Cryptocurrencies and the downside risk in equity investments. *Financ Res Lett* 33: 101211. https://doi.org/10.1016/j.frl.2019.06.009

Corbet S, Lucey B, Yarovaya L (2018) Datestamping the Bitcoin and Ethereum bubbles. *Financ Res Lett* 26: 81–88. https://doi.org/10.1016/j.frl.2017.12.006

Council F (2021) The Main Roadblocks to Crypto Moving Mainstream. Available from: https://www.forbes.com/sites/forbesbusinesscouncil/2021/06/23/the-main-roadblocks-to-crypto-moving-mainstream/?sh=2e629de922b9.

Dempster AP, Laird NM, Rubin DB (1977) Maximum Likelihood from Incomplete Data Via the *EM* Algorithm. *J R Stat Soc B* 39: 1–22. https://doi.org/10.1111/j.2517-6161.1977.tb01600.x

Dickey DA, Fuller WA (1979) Distribution of the Estimators for Autoregressive Time Series with a Unit Root. *J Am Stat Assoc* 74: 427. https://doi.org/10.2307/2286348

Dickey DA, Fuller WA (1981) Likelihood Ratio Statistics for Autoregressive Time Series with a Unit Root. *Econometrica* 49: 1057. https://doi.org/10.2307/1912517

Dimri SC, Indu R, Negi HS, et al. (2024) Hidden Markov Model—Applications, Strengths, and Weaknesses. *2024 2nd International Conference on Device Intelligence, Computing and Communication Technologies (DICCT)*, 300–305. https://doi.org/10.1109/DICCT61038.2024.10532827

Eirola E, Lendasse A (2013) Gaussian Mixture Models for Time Series Modelling, Forecasting, and Interpolation. In: A. Tucker, F. Höppner, A. Siebes, & S. Swift (Eds.), *Advances in Intelligent Data Analysis XII*, 162–173. Springer Berlin Heidelberg. https://doi.org/10.1007/978-3-642-41398-8_15

Engle RF (1982) Autoregressive Conditional Heteroscedasticity with Estimates of the Variance of United Kingdom Inflation. *Econometrica* 50: 987. https://doi.org/10.2307/1912773

Engle RF, Manganelli S (2004) CAViaR: Conditional Autoregressive Value at Risk by Regression Quantiles. *J Bus Econ Stat* 22: 367–381. https://doi.org/10.1198/073500104000000370

Esmael B, Arnaout A, Fruhwirth RK, et al. (2012) Improving time series classification using Hidden Markov Models. *2012 12th International Conference on Hybrid Intelligent Systems (HIS)*, 502–507. https://doi.org/10.1109/HIS.2012.6421385

Figá-Talamanca G, Patacca M (2019) Does market attention affect Bitcoin returns and volatility? *Decis Econ Financ* 42: 135–155. https://doi.org/10.1007/s10203-019-00258-7

Figà-Talamanca G, Focardi S, Patacca M (2021) Regime switches and commonalities of the cryptocurrencies asset class. *North Am J Econ Financ* 57: 101425. https://doi.org/10.1016/j.najef.2021.101425

Foroni B, Merlo L, Petrella L (2024) Expectile hidden Markov regression models for analyzing cryptocurrency returns. *Stat Comput* 34: 66. https://doi.org/10.1007/s11222-023-10377-2

Gershman SJ, Blei DM (2011) A Tutorial on Bayesian Nonparametric Models (Version 2). *arXiv*. https://doi.org/10.48550/ARXIV.1106.2697

Gonçalves S, Kilian L (2004) Bootstrapping autoregressions with conditional heteroskedasticity of unknown form. *J Econometrics* 123: 89–120. https://doi.org/10.1016/j.jeconom.2003.10.030

Granger CWJ (1969) Investigating Causal Relations by Econometric Models and Cross-spectral Methods. *Econometrica* 37: 424. https://doi.org/10.2307/1912791

Guesmi K, Saadi S, Abid I, et al. (2019) Portfolio diversification with virtual currency: Evidence from bitcoin. *Int Rev Financ Anal* 63: 431–437. https://doi.org/10.1016/j.irfa.2018.03.004

Hadan H, Zhang-Kennedy L, Nacke L, et al. (2024) Comprehending the Crypto-Curious: How Investors and Inexperienced Potential Investors Perceive and Practice Cryptocurrency Trading. *Int J Human–Comput Interact* 40: 5675–5696. https://doi.org/10.1080/10447318.2023.2239556

Hamilton JD (1989) A New Approach to the Economic Analysis of Nonstationary Time Series and the Business Cycle. *Econometrica* 57: 357. https://doi.org/10.2307/1912559

Hamilton JD (1994) *Time Series Analysis*. Princeton University Press.

Ji Q, Bouri E, Gupta R, et al. (2018) Network causality structures among Bitcoin and other financial assets: A directed acyclic graph approach. *Q Rev Econ Financ* 70: 203–213. https://doi.org/10.1016/j.qref.2018.05.016

Johnson MJ, Willsky AS (2013) Bayesian Nonparametric Hidden Semi-Markov Models. *J Mach Learn Res* 14: 673–701. Available from: https://www.jmlr.org/papers/volume14/johnson13a/johnson13a.pdf.

Kalliovirta L, Meitz M, Saikkonen P (2016) Gaussian mixture vector autoregression. *J Econometrics* 192: 485–498. https://doi.org/10.1016/j.jeconom.2016.02.012

Katsiampa P, Corbet S, Lucey B (2019) Volatility spillover effects in leading cryptocurrencies: A BEKK-MGARCH analysis. *Financ Res Lett* 29: 68–74. https://doi.org/10.1016/j.frl.2019.03.009

Kim K, Lee SYT, Assar S (2022) The dynamics of cryptocurrency market behavior: Sentiment analysis using Markov chains. *Ind Manage Data Syst* 122: 365–395. https://doi.org/10.1108/IMDS-04-2021-0232

Kochliaridis V, Papadopoulou A, Vlahavas I (2024) UNSURE - A machine learning approach to cryptocurrency trading. *Appl Intell* 54: 5688–5710. https://doi.org/10.1007/s10489-024-05407-z

Koenker R, Bassett G (1978) Regression Quantiles. *Econometrica* 46: 33. https://doi.org/10.2307/1913643

Lee S, Kim C (2023) Dirichlet process mixture models using matrix-generalized half-t distribution. *Stat* 12: e599. https://doi.org/10.1002/sta4.599

Li B (2023) Hidden Markov Model Based Stock Price Prediction: A Financial Research Report Based on Big Data Technology. *SSRN Electronic J*. https://doi.org/10.2139/ssrn.4622722

Ljung GM, Box GEP (1978) On a measure of lack of fit in time series models. *Biometrika* 65: 297–303. https://doi.org/10.1093/biomet/65.2.297

Ma F, Liang C, Ma Y, et al. (2020) Cryptocurrency volatility forecasting: A Markov regime-switching MIDAS approach. *J Forecast* 39: 1277–1290. https://doi.org/10.1002/for.2691

Merlo L, Petrella L, Raponi V (2021) Forecasting VaR and ES using a joint quantile regression and implications in portfolio allocation. *J Bank Financ* 133: 106248. https://doi.org/10.48550/ARXIV.2106.06518

Meunier S (2018) Blockchain 101. In: *Transforming Climate Finance and Green Investment with Blockchains*, 23–34. Elsevier. https://doi.org/10.1016/B978-0-12-814447-3.00003-3

Mgadmi N, Béjaoui A, Moussa W (2023) Disentangling the Nonlinearity Effect in Cryptocurrency Markets During the Covid-19 Pandemic: Evidence from a Regime-Switching Approach. *Asia-Pac Financ Mark* 30: 457–473. https://doi.org/10.1007/s10690-022-09384-6

Mgadmi N, Sadraoui T, Abidi A (2024) Causality between stock indices and cryptocurrencies before and during the Russo–Ukrainian war. *Int Rev Econ* 71: 301–323. https://doi.org/10.1007/s12232-023-00444-5

Morkūnaitė I, Celov D, Leipus R (2024) Evaluation of Value-at-Risk (VaR) using the Gaussian Mixture Models. *Res Stat* 2: 2346075. https://doi.org/10.1080/27684520.2024.2346075

Mungo L, Bartolucci S, Alessandretti L (2024) Cryptocurrency co-investment network: Token returns reflect investment patterns. *EPJ Data Sci* 13: 11. https://doi.org/10.1140/epjds/s13688-023-00446-x

Oelschläger L, Adam T (2023) Detecting bearish and bullish markets in financial time series using hierarchical hidden Markov models. *Stat Model* 23: 107–126. https://doi.org/10.1177/1471082X211034048

Pennoni F, Bartolucci F, Forte G, et al. (2022) Exploring the dependencies among main cryptocurrency log-returns: A hidden Markov model. *Economic Notes* 51: e12193. https://doi.org/10.1111/ecno.12193

Reynolds D (2009) Gaussian Mixture Models. In: S. Z. Li & A. Jain (Eds.), *Encyclopedia of Biometrics,* 659–663. Springer US. https://doi.org/10.1007/978-0-387-73003-5_196

Scrucca L (2024) Entropy-Based Volatility Analysis of Financial Log-Returns Using Gaussian Mixture Models. *Entropy* 26: 907. https://doi.org/10.3390/e26110907

Sims CA (1980) Macroeconomics and Reality. *Econometrica* 48: 1. https://doi.org/10.2307/1912017

Statista (2025) Biggest cryptocurrency in the world—both coins and tokens—based on market capitalization on February 25, 2025 (in billion U.S. dollars), *Statista*. Available from: https://www.statista.com/statistics/1269013/biggest-crypto-per-category-worldwide/.

Tan K, Chu M (2012) Estimation of Portfolio Return and Value at Risk Using a Class of Gaussian Mixture Distributions. *Int J Bus Financ Res* 6: 97–107. Available from: https://access.portico.org/stable?au=phx4jw4b1n4.

Taylor JW (2019) Forecasting Value at Risk and Expected Shortfall Using a Semiparametric Approach Based on the Asymmetric Laplace Distribution. *J Bus Econ Stat* 37: 121–133. https://doi.org/10.1080/07350015.2017.1281815

Tengelin K, Sopasakis A (2020) Tick based clustering methodologies establishing support and resistance levels in the currency exchange market. *Natl Account Rev* 2: 354–366. https://doi.org/10.3934/NAR.2020021

Turatti DE, Mendes FHPS, Mazzeu JHG (2025) Combining Volatility Forecasts of Duration-Dependent Markov-Switching Models. *J Forecast* 44: 1195–1210. https://doi.org/10.1002/for.3212

Wang Y, Andreeva G, Martin-Barragan B (2023) Machine learning approaches to forecasting cryptocurrency volatility: Considering internal and external determinants. *Int Rev Financ Anal* 90: 102914. https://doi.org/10.1016/j.irfa.2023.102914

Wang Y, Xu J, Huang SL, et al. (2025) Assessing Uncertainty in Stock Returns: A Gaussian Mixture Distribution-Based Method (Version 1). *arXiv*. https://doi.org/10.48550/ARXIV.2503.06929

White H, Kim TH, Manganelli S (2015) VAR for VaR: Measuring tail dependence using multivariate regression quantiles. *J Econometrics* 187: 169–188. https://doi.org/10.1016/j.jeconom.2015.02.004

Wong ACS, Chan WS (2005) Mixture Gaussian Time Series Modeling of Long-Term Market Returns. *North Am Actuar J* 9: 83–94. https://doi.org/10.1080/10920277.2005.10596227

Yi S, Xu Z, Wang GJ (2018) Volatility connectedness in the cryptocurrency market: Is Bitcoin a dominant cryptocurrency? *Int Rev Financ Anal* 60: 98–114. https://doi.org/10.1016/j.irfa.2018.08.012

Yuksel SE, Bolton J, Gader P (2015) Multiple-Instance Hidden Markov Models with Applications to Landmine Detection. *Ieee T Geosci Remote* 53: 6766–6775. https://doi.org/10.1109/TGRS.2015.2447576

Zhang MH, Cheng QS (2003) Gaussian mixture modelling to detect random walks in capital markets. *Math Comput Model* 38: 503–508. https://doi.org/10.1016/S0895-7177(03)90022-7

Zou Y, Lin Y, Song X (2024) Bayesian Heterogeneous Hidden Markov Models with an Unknown Number of States. *J Comput Graph Stat* 33: 15–24. https://doi.org/10.1080/10618600.2023.2231055